Understanding the catalytic conversion of automobile exhaust emissions using model catalysts: CO + NO reaction on Pd(111)

Emrah Ozensoy, Christian Hess*, and D. Wayne Goodman**

Department of Chemistry, Texas A&M University, P.O. Box 30012, College Station, TX 77842-3012

The CO + NO reaction is one of the profoundly important reactions that take place on Pd-based industrial three-way catalysts (TWC). In this review, we discuss results from polarization modulation infrared reflection absorption spectroscopy (PM-IRAS) and conventional IRAS experiments on CO adsorption, NO adsorption and the CO + NO reaction on a Pd(111) model catalyst surface within a wide range of pressures (10^{-6}–450 Torr) and temperatures (80–650 K). It will be shown that these studies allow for a detailed understanding of the adsorption behavior of these species as well as the nature of the products that are formed during their reaction under realistic catalytic conditions. CO adsorption experiments on Pd(111) at elevated pressures reveal that CO overlayers exhibit similar adsorption structures as found for ultrahigh vacuum (UHV) conditions. On the other hand, in the case of the CO + NO reaction on Pd(111), the pressure dependent formation of isocyanate containing species' was observed. The importance of this observation and its effects on the improvement of the catalytic NO_x abatement is discussed. The kinetics of the CO + NO reaction on Pd(111) were also investigated and the factors affecting its selectivity are addressed.

KEY WORDS: Pd; CO; NO; NO_x; infrared; TWC; Pd(111); isocyanate; –NCO

1. Introduction

In the last few decades, the constant increase in the number of environmental protection regulations world wide has brought about significant restrictions on the nature and the quantity of the exhaust gases originating from mobile sources such as automobile emissions. These increasingly demanding criteria for exhaust emissions led to an intense scientific interest in the development of catalytic converters with higher performance and longer lasting stability. Pt/Rh (90/10) three-way catalysts (TWC) that simultaneously oxidize CO to CO_2, reduce NO_x to N_2 and combust unburned hydrocarbons [1] were developed in 1970s as an initial solution for this technological problem. In the mid-1990s, Pd-only TWCs consisting of Pd particles deposited on a high surface area metal-oxide support (typically γ-Al_2O_3) containing varying amounts of stabilizers and/or promoters such as CeO_2, SiO_2, La_2O_3, and BaO were introduced as an alternative to Pt/Rh (90/10) catalyst. Pd rapidly became the most highly consumed precious metal by the automobile industry for emission control purposes due to its technical and economical advantages [2].

A detailed understanding of the fundamental chemical and physical phenomena that take place on the active sites of the catalysts as well as on the catalyst supports at the molecular level is crucial in order to design heterogeneous catalysts with higher performance. Therefore, properties of the Pd based model heterogeneous catalyst systems for gas/solid interfaces have been investigated extensively in our laboratories [3–49; D. Meier *et al.*, submitted; E. Ozensoy *et al.*, submitted]. Particularly, Pd single crystal surfaces [3–20; D. Meier *et al.*, submitted] Pd/X bimetallic systems (X = Mo [21–24], Ru [25–28], Cu [27,29], Ta [24,28,30], W [24,28,31,32], Re [24–26,28]), Pd/X/Y trimetallic systems (X/Y = Cu/Mo [33], Au/Mo [33]), Pd clusters deposited on SiO_2 [10,34–39; E. Ozensoy *et al.*, submitted], Al_2O_3 [40–45], TiO_2 [46–49] and MgO [47,49] have been examined using various surface spectroscopic tools.

Surface specific vibrational spectroscopic techniques are exceptionally well-suited tools for elucidating heterogeneous catalytic reaction mechanisms as they provide unique possibilities to identify active species on the catalyst surface with sub-monolayer accuracy and enable an *in situ* analysis of catalysts under reaction conditions, in real time. In this respect, infrared reflection absorption spectroscopy (IRAS) [7,9,50–52], polarization modulation infrared reflection absorption spectroscopy (PM-IRAS) [17,19,20; E. Ozensoy *et al.*, submitted, in preparation], high resolution electron energy loss spectroscopy (HREELS) [53–57], sum frequency generation (SFG) [58], and derivatives of these techniques [59] have been frequently used. In the current report, we discuss our vibrational spectroscopic results regarding the CO and NO adsorption as well as the mechanism and kinetics of the CO + NO reaction on Pd-based model catalysts, which have been extended to elevated pressure conditions only recently using *in situ* PM-IRAS [17,19,20; E. Ozensoy *et al.*, in preparation]. The adsorption of CO [18,50,60–67] NO [53–55,68–84] as well as the CO + NO reaction [20,85–106] on Pd-

* Current address: Fritz-Haber-Institut der Max-Planck-Gesellschaft, Abteilung Anorganische Chemie, Faradayweg 4-6, D-14195 Berlin, Germany.

** To whom correspondence should be addressed. E-mail: goodman@mail.chem.tamu.edu

1022-5528/04/0400–0013/0 © 2004 Plenum Publishing Corporation

based catalysts have been thoroughly investigated by other groups also, both experimentally and theoretically [107–118].

The outline of this report is as follows: Section 2 briefly describes the experimental techniques that are utilized in our studies. Basically, our approach to obtain a fundamental understanding of the complex surface phenomena is to start with simple but atomically well-defined model systems that can be studied with high experimental accuracy. We then increase the complexity of the examined model catalyst system in a controlled manner to mimic crucial aspects of a realistic/working heterogeneous catalyst. Therefore, Section 3 starts with the investigation of the adsorption behavior of each of the reactants of the CO + NO reaction on the atomically flat Pd(111) single crystal surface, both under ultrahigh vacuum (UHV) and elevated pressure conditions (~450 Torr) using PM-IRAS and conventional IRAS, respectively. As has been demonstrated previously in our group, Pd particles supported by SiO_2 [36] and Al_2O_3 [40] ultra-thin films exhibit mostly <111> facets (with a minor contribution from <100> facets). Therefore, in the present discussion, we will mostly focus on results obtained for the Pd(111) single crystal surface. Next, our IRAS results on the CO + NO coadsorption and reaction on Pd(111) model catalysts under low pressure conditions (typically $\sim 1 \times 10^{-6}$ Torr) are discussed. Results of these initial low-pressure studies were also compared with the analogous experiments at elevated pressure conditions (~180 Torr), where isocyanate formation is observed. In addition, dependence of the isocyanate formation on the total reactant pressure during the CO + NO reaction on Pd(111) is discussed and the implications of this observation on the catalytic NO_x removal are also addressed.

2. Experimental

The surface analysis chambers that have been utilized are UHV chambers coupled to a micro-reactor for *in situ* vibrational spectroscopic and kinetic studies. They include standard surface science techniques such as IRAS, PM-IRAS, Auger electron spectroscopy (AES), low energy electron diffraction (LEED) and temperature programmed desorption (TPD) spectroscopy. Pd single crystals were cleaned by performing repeated cycles of low temperature oxidation and subsequent high temperature annealing until the surfaces were found to be free of carbon, oxygen and sulfur contaminations as measured by AES.

PM-IRAS is a very versatile and a powerful *in situ* vibrational spectroscopic technique which can be applied to analyze surface properties of gas/solid interfaces at pressures close to atmospheric pressures with virtually no contribution from the gas phase species [17,19,20; E. Ozensoy *et al.*, submitted]. Briefly, the PM-IRAS setup used in this study consists of an infrared spectrometer (Bruker Equinox 55), a static wire-grid polarizer and a photoelastic modulator (PEM, Hinds instruments) to create a fast modulation of the polarization state of the incident light (ideally between s and p states). A demodulator-multiplexer electronics (GWC instruments, Bruker) is used to compute a differential reflectivity spectrum from the sum (p + s) and difference (p − s) signals collected by the mercury cadmium telluride (MCT) detector (figure 1). For the NO adsorption and CO + NO experiments described below the PEM controller was set to 1700 cm^{-1}, whereas it was set to 1800 cm^{-1} for the CO adsorption experiments. Data acquisition time for each of the PM-IRA spectra presented here was 4.5 min/spectra with a spectral resolution of 4 cm^{-1} for the CO/Pd(111) experiments

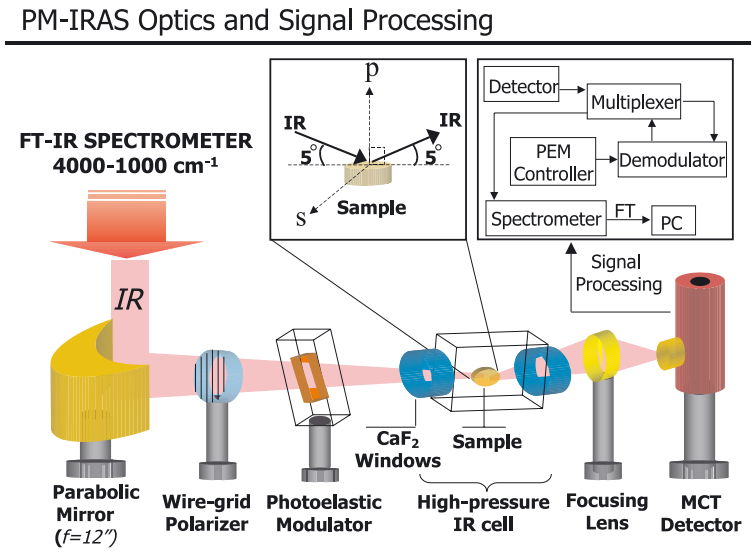

Figure 1. Schematic depicting the optical and electronic components of the PM-IRAS experimental setup.

and 8 cm^{-1} for the NO/Pd(111) and CO + NO/Pd(111) experiments.

CO, O_2, CO_2 and N_2O gases used in the experiments were of 99.99% purity or better, and the NO gas was C.P. grade. For the isotope experiments ^{13}CO (99%) and ^{15}NO (99%) were used. For CO adsorption experiments, CO was further purified using liquid nitrogen cold traps. This method allows the cleaning of CO up to 600 mbar, the vapor pressure of CO at 90 K. Purification of CO for pressures greater than 600 mbar was carried out using a *n*-pentane/liquid nitrogen slurry maintained at 143 K. Similarly, for NO adsorption and CO + NO reaction experiments, CO and NO gases were also purified using a *n*-pentane/liquid nitrogen slurry. To avoid any photo-induced NO_2 formation in the CO + NO gas mixture, both the premixing/cleaning procedures and the experiments were conducted with the exclusion of visible light.

The CO + NO reaction was performed in batch mode and the product formation was followed with infrared spectroscopy by monitoring both the adsorption behavior on the Pd surface (*via* PM-IRAS) and the evolution of the gas phase CO_2 and N_2O. The gas phase production of CO_2 and N_2O was calculated by converting infrared intensities into pressures by using a set of calibration curves. Turnover frequencies (TOF) were obtained by normalizing the gas phase production per second to the total number of surface sites.

For further experimental details, the reader is referred to our previous reports [7–10,13,17,19,20].

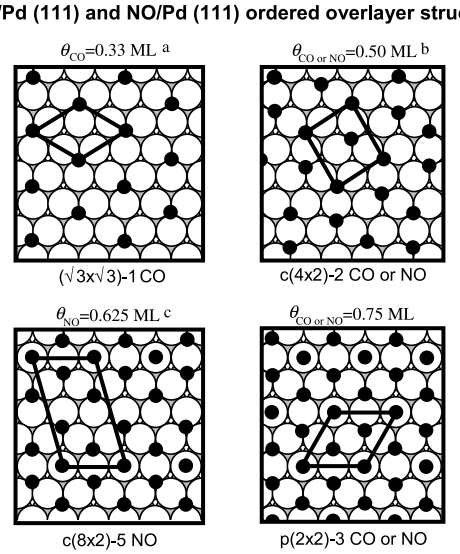

Figure 2. Structures of the ordered overlayers that are formed during NO or CO adsorption on the Pd(111) single crystal surface (see text for details). (a) This structure is only observed for CO. NO forms a disordered phase at $\theta_{NO} = 0.33$ ML [121]. (b) A similar phase with bridging adsorption was also proposed for CO/Pd(111) at $\theta_{CO} = 0.33$ ML. (c) Complex overlayer structures were reported for CO/Pd(111) at this coverage where mostly bridging sites are occupied [62].

3. Results and discussion

3.1. CO adsorption on Pd(111)

Coverage-dependent ordered overlayers of CO on Pd(111) single crystal surfaces have been studied extensively in the literature [7,50,60,62]. Vibrational spectroscopy, in particular the C—O stretching frequency of adsorbed CO can be used for adsorption site assignments of these ordered CO layers by comparing these values with the inorganic metal-carbonyl analogues where the coordination of CO to the metal center is accurately known. Although this approach was criticized as misleading in some specific cases [60,70,119], it is found to be very useful for many other systems where site assignments *via* vibrational spectroscopy can be verified with other complementary methods [50,62,120].

At a CO coverage of $\theta_{CO} = 0.33$ ML (ML = monolayer), recent STM studies suggest that CO on Pd(111) forms overlayers with a $(\sqrt{3} \times \sqrt{3})$ R 30°-1CO structure [62], occupying primarily threefold hollow adsorption sites (figure 2). Using a combination of LEED and IRAS techniques it was previously demonstrated that this CO overlayer yields a distinctly low C—O vibrational frequency of ~1850 cm^{-1} (figure 3a) [7,50]. As the CO coverage is further increased to $\theta_{CO} = 0.50$ ML, the adsorbed CO molecules exhibit two coexisting c(4×2)-2CO phases (figure 2), where CO occupies either the bridging sites or threefold hollow sites [62]. These structures correspond to a C—O vibrational frequency of ~1920 cm^{-1} [7,50]. Within $\theta_{CO} = 0.50$–0.75 ML, various complex overlayer structures have been reported [62], which result in a CO vibrational band near 1965 cm^{-1} [50]. Recent STM experiments combined with density functional theory (DFT) calculations suggest that CO occupies primarily bridging sites on the Pd(111) surface within this coverage regime [62]. Eventually, at $\theta_{CO} = 0.75$ ML, the CO saturation coverage is obtained yielding a (2×2)-3CO structure (figure 2). Within this structure, CO resides on both atop and threefold hollow sites corresponding to vibrational bands at 2110 and 1895 cm^{-1}, respectively (figure 3a) [7,50]. These adsorption site assignments for the CO/Pd(111) system at low pressures (~1×10^{-8} Torr) have been confirmed by the combined STM and DFT studies of Rose *et al.* [62].

The adsorption of CO on Pd(111) was also investigated at elevated pressures using PM-IRAS [19]. In this recent study (see figure 3b) [19] it was demonstrated that CO overlayers follow similar trends in terms of the observed vibrational frequencies within 10^{-6}–450 Torr (i.e. within a dynamic pressure range of nine orders of magnitude!), implying that no new pressure-induced species nor adsorbate-induced surface reconstructions occur on the Pd(111) surface during CO adsorption at elevated pressures. Therefore, an equilibrium phase

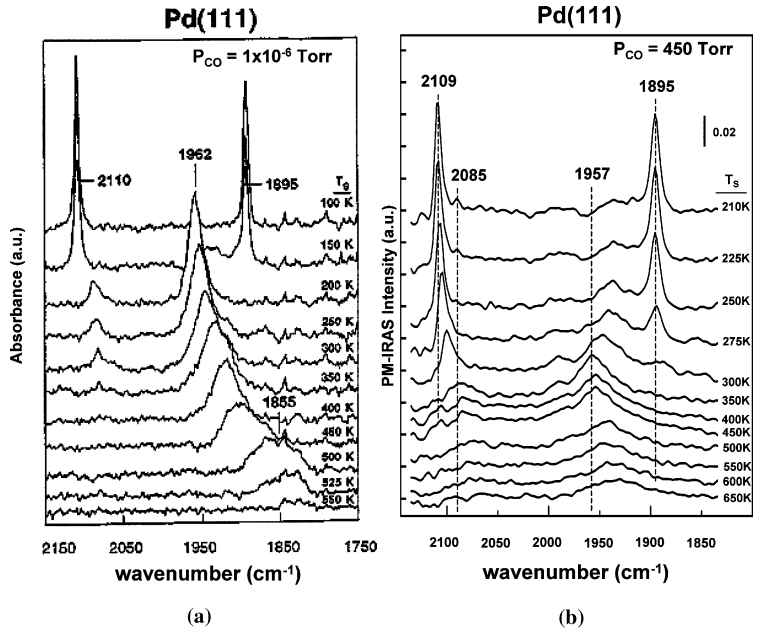

Figure 3. *In situ* IRA spectra for CO adsorption on Pd(111) at $P_{CO} = 1\times10^{-6}$ Torr (a) [7] and *in situ* PM-IRA spectra for CO adsorption on Pd(111) at $P_{CO} = 450$ Torr (b) [19]. All of the spectra are acquired *in the presence of the CO gas phase*. Initial adsorption was performed at the highest temperature given in each of the spectral series.

diagram was constructed showing the different types of Pd(111) sites that are occupied by adsorbed CO molecules at various pressure and temperature regimes (figure 4). Furthermore, a transition from a phase dominated by CO molecules adsorbed on bridging sites to a different phase where CO resides on atop/threefold hollow sites is monitored by varying the CO pressure within nine orders of magnitude. The apparent activation energy of this phase transition was calculated to be 44.3 kJ/mol (figure 4) [19].

The elevated pressure PM-IRAS results for the CO adsorption on the Pd(111) single crystal model catalyst discussed above provide important insights about the correlation between traditional surface science studies performed under UHV/low-temperature conditions and the real heterogeneous catalytic applications where elevated pressures and temperatures are employed. Our PM-IRAS results on CO adsorption on Pd(111) clearly indicate that UHV studies can be readily extrapolated to estimate the state of the examined catalytic system under more realistic conditions. These findings also demonstrate the wide-ranging experimental *in situ* capabilities offered by PM-IRAS which make it a powerful, yet experimentally straight forward technique that can be successfully applied to bridge the so-called *pressure gap* between surface science and heterogeneous catalysis.

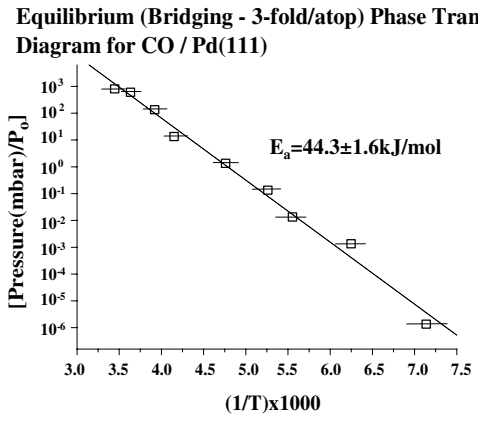

Figure 4. Isosteric plot for the phase transition from bridging to atop/threefold CO on Pd(111).

3.2. NO adsorption on Pd(111)

In terms of their coverage dependent ordered structures, NO overlayers on Pd(111) show striking similarities to the CO overlayers on Pd(111) (see figure 2) [8,53,55,70,72,81,103,121; E. Ozensoy *et al.*, in preparation]. In the literature, a c(4×2) phase at $\theta_{NO} = 0.5$ ML [8,55,72,121], which transforms into an ordered phase with a c(8×2) structure at $\theta_{NO} = 0.625$ ML [8] was reported, in addition to the p(2×2) overlayer at the NO saturation coverage of $\theta_{NO} = 0.75$ ML [8,55,72]. Besides these ordered structures, another overlayer structure, which lacks long range order, was also reported for low NO coverages ($\theta_{NO} = 0.33$ ML) [55,72,121]. It should be noted that there has been a long-standing controversy regarding the adsorption site assignments for these NO overlayers using vibrational spectroscopic techniques [70]. For instance, the adsorption sites for the c(4×2) structure that was originally associated with the bridging

sites [8,55,72] were assigned to atop sites in a later study [103]. On the other hand, DFT studies proposed that NO occupies threefold hollow [114] or threefold hollow + atop [73] sites in this phase.

A recent report by Hansen *et al.* [73], which combines atomic resolution STM and DFT calculation studies seems to resolve this long-standing controversy. By employing these two powerful methods, the authors suggest that NO molecules reside on the threefold hollow (fcc and hcp) sites in the c(4×2)-2NO domains (figure 2). In the c(8×2)-5NO domains, each NO overlayer unit cell consists of four NO molecules occupying fcc and hcp threefold sites in addition to one NO molecule on the atop sites (figure 2). It was also argued in the same study that NO molecules on the atop sites are tilted with respect to the surface normal in the c(8×2)-5NO phase. For the p(2×2)-3NO domains, they propose a unit cell structure where one NO molecule occupies atop sites with a tilted orientation with two other NO molecules sitting on the threefold hollow sites (fcc and hcp). Another important observation regarding the NO/Pd(111) adsorption system in this report is the simultaneous coexistence of different ordered NO overlayers on the Pd(111) surface. STM results [73] reveal that at a coverage regime where a complete c(8×2)-5NO overlayer is expected, NO molecules on Pd(111) *always* exist as separate coexisting domains of c(8×2)-5NO, c(4×2)-2NO and p(2×2)-3NO. This observation was explained using the adsorption energetics of the different NO overlayers. Due to the repulsive interaction between the adsorbed NO molecules on Pd(111), the NO chemisorption energy is found to be monotonically decreasing with increasing coverage [73]. In other words, the NO chemisorption potential for the p(2×2)-3NO phase is lower than for the c(8×2)-5NO phase, whereas the NO chemisorption potential for c(4×2)-2NO is higher than that of the c(8×2)-5NO domains. Thus the total energy of the NO/Pd(111) system with a complete c(8×2)-5NO overlayer can also be reached by having separate domains of (8×2)-5NO, c(4×2)-2NO and p(2×2)-3NO overlayers existing simultaneously.

Vibrational spectroscopic results [8,55; E. Ozensoy *et al.*, in preparation] for NO/Pd(111) can be interpreted more accurately in the light of the information provided by these recent STM and DFT studies [73]. Figure 5a [8] shows the IRAS results obtained for the NO/Pd(111) system at low pressures ($P_{NO} \sim 1 \times 10^{-6}$ Torr). At a NO coverage of $\theta_{NO} = 0.5$ ML, a LEED pattern corresponding to a c(4×2)-2NO structure is obtained. At the same coverage a N—O stretching band at 1620 cm^{-1} is observed. Based on the arguments given above, this adsorption band can be assigned to NO molecules residing on threefold hollow sites. As the NO coverage is increased, a red shift in the NO band (corresponding to threefold hollow sites) to 1615 cm^{-1} is observed. In addition, another high frequency adsorption band around 1734 cm^{-1} appears that can be attributed to NO bound to atop sites. When a NO coverage of $\theta_{NO} = 0.625$ ML is reached, a LEED pattern suggesting a c(8×2)-5NO phase is obtained. NO bands at 1744 and 1736 cm^{-1} are observed corresponding to NO species at different atop adsorption sites. Two other low frequency bands at ~1605 and 1586 cm^{-1} correspond to adsorption on threefold hollow sites. As the previous STM studies suggest that the c(8×2)-5NO phase always coexists with the c(4×2)-2NO and p(2×2)-3NO domains [73], the IRA spectrum for the (8×2) phase should indeed be a convolution of all these three separate domains. This argument provides a new interpretation for the spectrum in figure 5a, suggesting that the shoulder at ~1605 cm^{-1} can be associated with the NO molecules sitting on the threefold hollow sites of c(4×2)-2NO domains. Similarly the high frequency adsorption band at 1744 cm^{-1} can be attributed to NO species occupying atop sites of

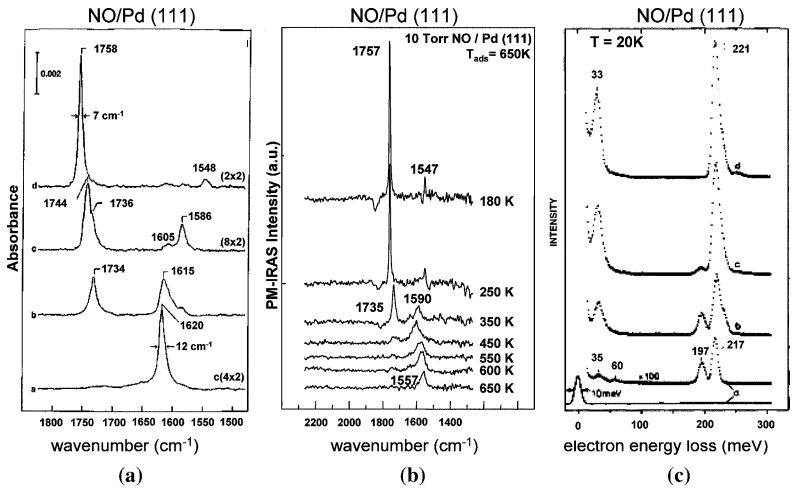

Figure 5. (a) IRAS data representative of the ordered overlayers of NO on Pd(111) obtained at $P_{NO} \sim 10^{-6}$ Torr [8]. (b) PM-IRA spectra for NO adsorption on Pd(111) at 10 Torr (E. Ozensoy *et al.*, in preparation). (c) HREEL spectra for low temperature (20 K) NO adsorption on Pd(111) with increasing NO coverage and NO-dimer formation [55].

p(2×2)-3NO domains. Then the remaining two features at 1736 and 1586 cm^{-1} can be readily assigned to NO species adsorbed on atop and threefold hollow sites of c(8×2)-5NO domains, respectively.

At a saturation coverage of $\theta_{NO} = 0.75$ ML, a p(2×2)-3NO overlayer structure is formed as confirmed by the LEED images [8] and the IRAS data yield two distinct NO adsorption bands at 1758 and 1548 cm^{-1} due to atop and threefold hollow adsorption, respectively. An interesting aspect of the topmost IRA spectrum in figure 5a is the relative IR intensity of the NO species corresponding to atop and threefold hollow sites. As the p(2×2)-3NO unit cell structure implies the presence of two NO molecules adsorbed on hollow sites for every NO molecule sitting on the atop sites, the smaller IRAS intensity for the NO molecules residing on the hollow sites with respect to the atop sites suggests that the IRAS cross sections for these two adsorbed states should be considerably different. This well known effect is demonstrated in a recent DFT study [122] where it was shown that the IR cross sections for CO molecules on atop and hollow sites of Pd(111) may vary by a factor of four as a function of the coverage-dependent overlayer structure. Figure 5b shows the PM-IRAS results (E. Ozensoy *et al.*, in preparation) for NO adsorption on Pd(111) at elevated pressures ($P_{NO} = 10$ Torr). It is clearly seen that the vibrational adsorption bands for NO follow similar trends from 10^{-6} up to 10 Torr. Further details of the elevated pressure experiments on the NO/Pd(111) adsorption system will be discussed in a forthcoming publication (E. Ozensoy *et al.*, in preparation).

It has been demonstrated previously that at lower adsorption temperatures such as 20 K, in addition to the previously mentioned NO species, a new NO adsorption band at 1782 cm^{-1} (221 meV) is observed on Pd(111) using HREELS [121], which displays a shoulder at ~1860 cm^{-1} (230 meV) (figure 5c). These two low-temperature NO bands (221 and 230 meV) were attributed to the asymmetric and symmetric stretching modes of a weakly bound NO-dimer species ($(NO)_2$), respectively. The formation of NO-dimer species has also been observed in recent PM-IRAS studies on the NO/Pd(111) adsorption system at elevated pressures (E. Ozensoy *et al.*, in preparation). Observation of $(NO)_2$ species on Pd(111) deserves special attention as it has been shown in the literature that N_2O is formed on Ag(111) *via* an $(NO)_2$ intermediate [70].

The dissociation of NO on Pd(111) at high temperatures (373–518 K) has also been investigated by HREELS [53] and TPD [13,53] under UHV conditions. HREELS studies reveal that NO desorbs mostly molecularly from the Pd(111) surface around 500 K with a small amount of dissociation above 490 K [53]. However, it was reported that NO dissociation is significantly facilitated in the presence of surface steps such as in the case of the stepped Pd(112) surface [53]. In case of Pd(111), atomic O species formed (due to NO dissociation) are detected only up to 550 K [53]. Above this temperature, atomic O is reported to dissolve into the bulk to form subsurface O. No O_2 was detected in TPD studies of NO desorption from a Pd(111) surface although other dissociation products such as NO, N_2 and N_2O were readily observed [13,53].

3.3. CO + NO coadsorption and reaction on Pd(111)

3.3.1. CO + NO reaction on Pd(111) at low pressures

As discussed above, the CO/Pd(111) and NO/Pd(111) adsorption systems are now understood in great detail. In the following section, the more complex interaction of CO and NO during the CO + NO reaction on the Pd(111) model catalyst is addressed. Figure 6 [13] presents temperature dependent IRAS results for CO + NO coadsorption on a Pd(111) single crystal model catalyst surface ($P_{CO+NO} = 1\times10^{-6}$ Torr, $P_{CO}/P_{NO} = 1$). The series of spectra in figure 6 reveals that CO occupies predominantly threefold hollow sites (~1915 cm^{-1}) under both low and high temperature conditions, whereas NO prefers atop sites (1744 cm^{-1}) at low temperatures and threefold hollow sites (1576–1530 cm^{-1}) at high temperatures [13]. In addition, at the saturation coverage, NO and CO bands on Pd(111) have similar intensities, whereas at lower coverages NO

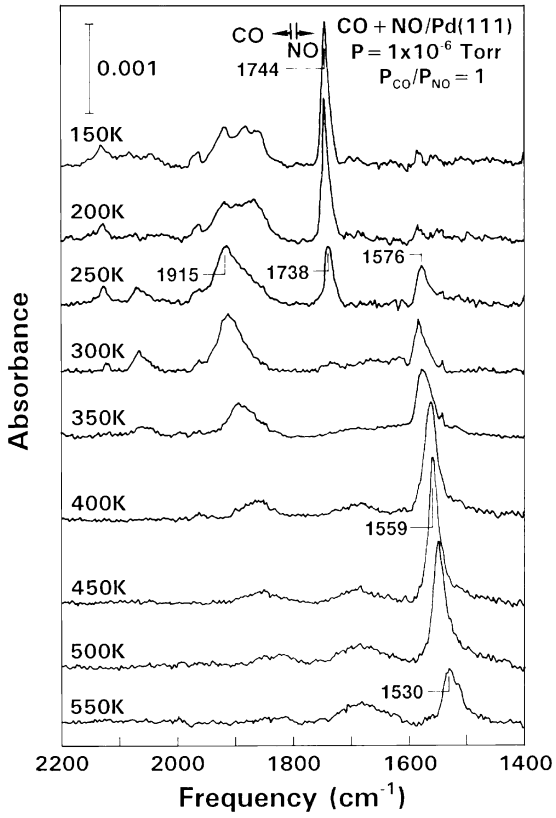

Figure 6. Low pressure IRA spectra for CO + NO coadsorption and reaction on Pd(111) where $P_{CO+NO} = 1\times10^{-6}$ Torr and $P_{CO}/P_{NO} = 1$ [10].

bands have a significantly higher intensity. This is consistent with recent theoretical calculations [110] suggesting that NO has a relatively higher adsorption energy at saturation coverage with respect to CO, whereas at low coverages these two adsorbates have similar adsorption energetics.

A comparative look at the IRAS data allows us to obtain important clues about the nature of the CO and NO adsorption on the transition metal surfaces. The Blyholder model [67] has been widely used to interpret the frequency shifts for CO adsorption bands in vibrational spectroscopic experiments. According to this model, CO binds to the metal surface *via* electron donation from its 5σ orbital that is accompanied by a backdonation from the metal $d\pi$ orbital to the empty $2\pi^*$ orbital of CO. As the CO coverage increases, depletion of the electron density of the metal d band results in a decreased back donation to the $2\pi^*$ orbital of CO which leads to a vibrational blue shift in the C—O stretching frequency. On the other hand, NO containing one more electron than CO in its $2\pi^*$ orbital, can form a covalent bond with the metal surface also through other models [123] such as spin pairing of the NO $2\pi^*$ electron with a metal $d\pi$ electron to form a covalent π bond. This is accompanied by electron donation from the NO 5σ orbital to an empty σ orbital of the metal to obtain a linear geometry or spin pairing of the NO $2\pi^*$ electron with a metal σ electron to assume a tilted geometry. In the latter case, only little donation from the NO 5σ orbital to the metal occurs. IRAS experiments [124] on CO + NO coadsorption on Pd(111) at 300 K, from the minimum detectable coverages to the saturation coverages, indicate that the frequency shift for the CO adsorption bands is +77 whereas the corresponding shift for NO is only +46 cm^{-1}, respectively. This marked difference in the magnitude of the coverage dependent vibrational blue shifts of NO compared to CO may suggest that the backdonation from the metal d band to the NO $2\pi^*$ orbitals may not necessarily be the prominent factor for the nature of the Pd—NO bond. However, $5\sigma/2\pi^*$ donation from NO to Pd may have a larger contribution to the observed frequency shifts. Thus with increasing NO coverage, the smaller degree of 5σ donation from NO to the metal may have only a small effect on the strength of the N—O bond as the 5σ orbital is only slightly antibonding (contrary to the CO $2\pi^*$ orbital). Hence the smaller coverage dependence of the N—O stretching frequency on Pd surfaces can be explained by the stabilization of the Pd—NO bond as a result of the primarily covalent bonding interaction [123].

3.3.2. CO + NO reaction on Pd(111) at elevated pressures and the formation of isocyanate

Recently, the CO + NO reaction has also been studied at elevated pressures using *in situ* PM-IRAS [17,20]. Figure 7 shows the PM-IRA spectra obtained in the presence of a total CO + NO pressure of 240 mbar (i.e. 180 Torr) with $P_{CO}:P_{NO} = 1.5$. Comparison of low (figure 6) and high pressure (figure 7) results for the CO + NO reaction on Pd(111) suggests that NO and CO occupy similar adsorption sites in both pressure regimes. Furthermore, CO_2 yields determined by gas phase IR spectroscopy (figure 8) suggest that the reaction rate is insignificant below 550 K. However, above this temperature, a drastic increase in the reaction rate is observed. Besides the anticipated CO and NO adsorption bands in figure 7, above 500 K, the development of another feature at 2256 cm^{-1} is also visible. Isotopic labeling experiments revealed that this broad and complex feature is associated with isocyanate (—NCO) containing species (mostly —NCO and HNCO with H originating from bulk of the Pd crystal) that are formed due to the reaction between adsorbed CO and atomic N, which is

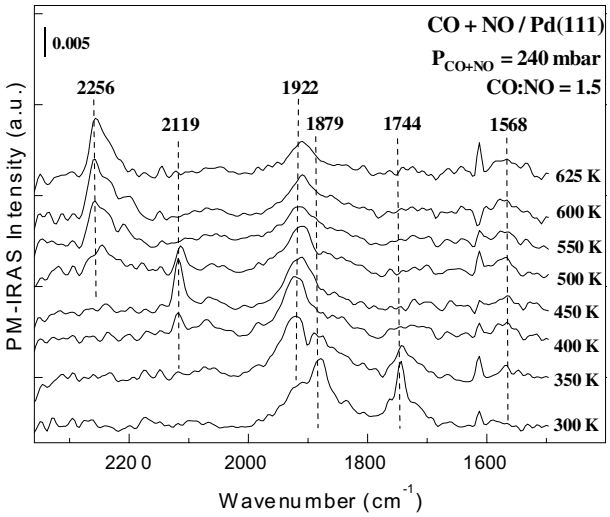

Figure 7. *In situ* PM-IRA spectra for CO + NO coadsorption and reaction on Pd(111) at 240 mbar (180 Torr), $P_{CO}/P_{NO} = 1.5$ [20].

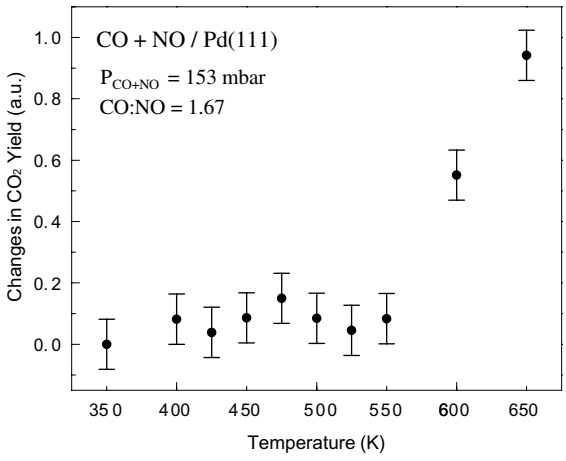

Figure 8. Relative CO_2 conversion versus temperature in CO + NO reaction on Pd(111) (each data point represented here was obtained by integrating CO_2 yield for a period of 5 min at each given temperature) [20].

Table 1
Comparison of the isocyanate group frequencies and isotope frequency shifts (in cm^{-1}) on Pd(111) and Cu(100)

	$^{14}N^{12}CO$	$^{14}N^{13}CO$	$^{15}N^{12}CO$	$^{13}CO—^{12}CO$	$^{15}NO—^{14}NO$
Cu(100)[a]	2198	2140	2192	−58	−6
Pd(111)[b]	2243	2178	2230	−65	−13

[a] Celio *et al.* [131].
[b] Ozensoy *et al.* [17]. For the CO + NO and CO + ^{15}NO mixtures P_{total} = 0.67 mbar ($CO/^{14,15}NO$ = 1.5), for the ^{13}CO + NO mixture P_{total} = 1.06 mbar ($^{13}CO/NO$ = 1.3). Mixtures were dosed at 600 K.

formed *via* dissociation of NO on Pd(111) (Table 1) [17]. —NCO formation in the CO + NO reaction on Pd catalysts have also been reported in the literature, both in experimental [86,87,125–129] and theoretical [92] studies. It has been suggested that —NCO is formed on the metal centers and then spills over to the oxide support [130]. Along these lines, Solymosi and Bansagi [130] reported that the vibrational features for —NCO species on supported metal particles strongly depend on the nature of the oxide but not on the type of the metal.

As the formation mechanism of NCO containing species' on Pd(111) implies NO dissociation their formation can be used as a sensitive indicator for the NO dissociation process, which is a crucial step in the CO + NO reaction. Detection of NCO related features at 500 K (see figure 7), where the CO + NO reaction is still relatively slow, suggests that NO dissociation may not be the limiting step at this temperature. A very interesting aspect of the formation of NCO containing species' on Pd(111) at elevated pressures was demonstrated by varying the total pressure of the CO + NO gas phase (figure 9) [17]. It was shown that formation of NCO related features are *only* detected at elevated pressures (above 0.02 mbar) emphasizing the profound significance of *in situ* investigations of heterogeneous catalytic reactions under realistic experimental conditions. Furthermore, dependence of the —NCO/HNCO formation on the relative ratio of the partial pressures of the reactants in CO + NO reaction was also examined. Figure 10 [20] shows that —NCO/HNCO formation is significantly enhanced when the partial pressure of CO is increased in the reactant mixture. Besides, NCO containing species' were found to be extremely stable on Pd(111). Once they are formed at $T > 500$ K they are found to be stable within 300–650 K and even after pumping out the reactant gases down to ~10^{-7} Torr at 300 K. These results are in contrast to the Rh(111) case where they are found that —NCO has a very short lifetime and decomposes to N_2 and CO even at room temperature in the absence of an oxide support [130].

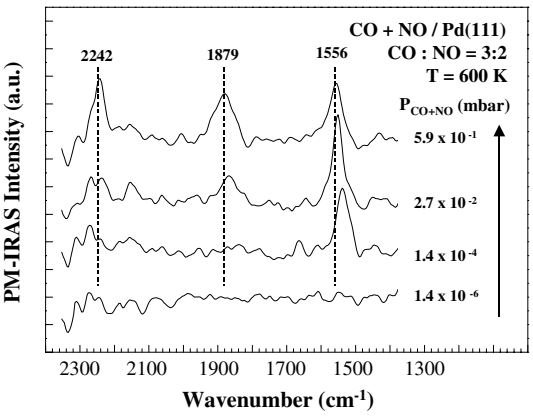

Figure 9. PM-IRAS data illustrating the pressure dependent formation of isocyanate containing species' during CO + NO reaction on Pd(111) [17].

The interesting chemistry of —NCO in the CO + NO reaction on platinum group metals deserves special attention as it was suggested that —NCO intermediate may provide important practical improvements in the catalytic NO_x abatement. Unland [125,126] proposed that in the presence excess of H_2O, NH_3 can also form during the CO + NO reaction on supported Pd catalysts *via* hydrolysis of an —NCO intermediate. Recently, Lambert and coworkers [127] studied CO + NO + H_2 + O_2 and CO + NO + H_2O reactions on a Pd/Al_2O_3 supported catalyst and showed the formation of NH_3 *via* hydrolysis of an —NCO intermediate. They suggested that NH_3 formation during these reactions may provide an additional route for NO_x removal as it eliminates the necessity for the addition of an external reducing agent such as NH_3. It was argued in the same study [127] that the performance of the H_2 + O_2 + CO + NO reactant mixture is superior to the H_2O + CO + NO mixture towards NH_3 formation on a high surface area Pd/Al_2O_3 catalysts. It was suggested that although NH_3 formation takes place through the hydrolysis of —NCO in both cases, H_2 adsorption on Pd particles may further weaken the N—O bond on Pd sites and thus enhance the NO dissociation and subsequent —NCO formation process. It should be also mentioned that in the presence of excess H_2, NH_3 formation can also readily occur *via* an alternative pathway which is the hydrogenation of atomic N. In a related study, Cant and coworkers [128,129] demonstrated the formation of gas phase HNCO in the CO + NO + H_2 reaction on high surface area Pd/SiO_2 and Pt/SiO_2 catalysts. This interesting finding supported the possibility that hydrolysis of —NCO to form NH_3 can take place *via* an HNCO intermediate as originally proposed by Unland [125].

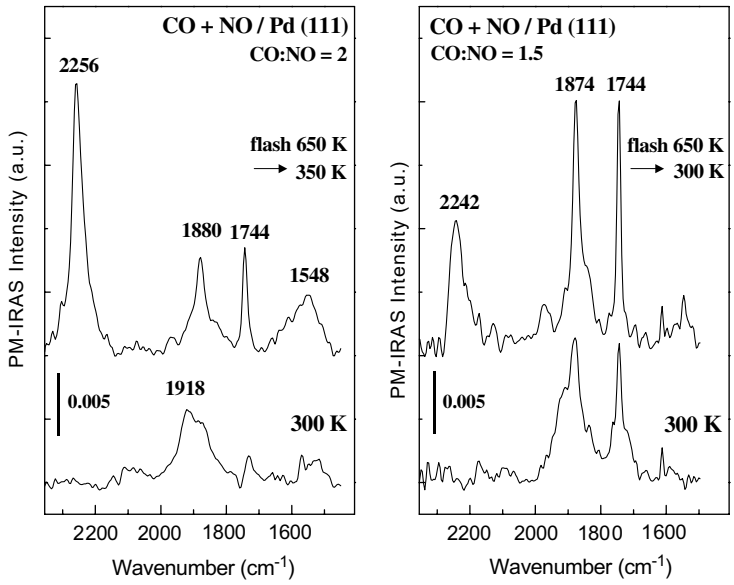

Figure 10. Influence of P_{CO}/P_{NO} partial pressure ratio on the amount of isocyanate containing species' on Pd(111) surface during CO + NO reaction [20].

Consequently, although —NCO/HNCO seems to be a spectator in CO + NO reaction on Pd(111), in the presence of large amounts of hydrogen containing species such as H_2 or H_2O, —NCO acts as an important intermediate on high surface area Pd catalysts to produce an additional reducing agent (NH_3) that can further enhance catalytic NO_x removal.

The temperature dependent selectivity of the CO + NO reaction on Pd(111) was also investigated at elevated pressures (figure 11) [20]. Some of the important factors which lead to the observed temperature dependence of N_2O selectivity can be explained by considering the branching ratio between the two major reaction pathways that have been suggested previously for the CO + NO reaction on Pd(111) [13,14,42]:

$$CO + NO \rightarrow CO_2 + \frac{1}{2}N_2 \quad (1)$$

$$CO + 2NO \rightarrow CO_2 + N_2O \quad (2)$$

Figure 11 illustrates that the N_2O selectivity monotonically increases with increasing temperature in the reaction regime (i.e. within 590–660 K). By looking at the series of spectra in figures 6 and 7, it can be realized that the relative concentrations of adsorbed NO to CO on the Pd(111) surface ($[NO]_{ads}/[CO]_{ads}$) also increase with increasing temperature in this temperature interval. As increasing $[NO]_{ads}/[CO]_{ads}$ forces pathway (2) to dominate, the N_2O selectivity increases with increasing temperature under reaction conditions.

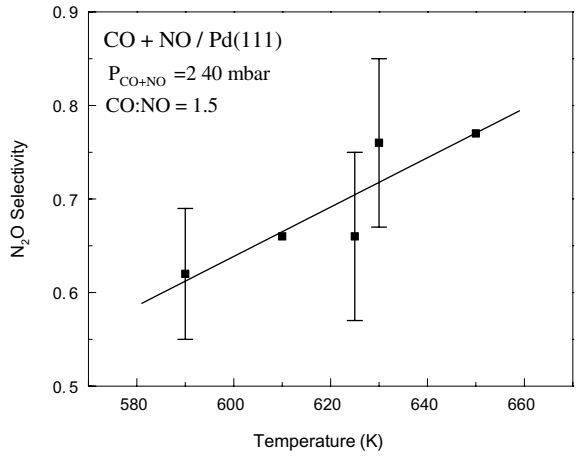

Figure 11. N_2O selectivities, $N_2O/(N_2 + N_2O)$, for the CO + NO reaction on Pd(111) at 240 mbar total pressure ($P_{CO}/P_{NO} = 1.5$) [20].

4. Conclusions

In this report we have addressed the CO adsorption, NO adsorption and CO + NO reaction on a Pd(111) single crystal model catalyst surface by discussing results from vibrational spectroscopic experiments obtained within a wide range of pressures and temperatures. In the case of the CO/Pd(111) adsorption system, we have demonstrated that the results of traditional surface scientific experiments under UHV conditions can be accurately extrapolated to the high-temperature/high-pressure regime even if the pressure differential between these two cases may be as large as 10^9. It was shown that similar coverage dependent CO overlayer structures are observed on Pd(111) without any indication for new pressure-induced species or occurrence of adsorbate-induced surface reconstructions at elevated pressures. On the other hand, by employing *in situ* PM-IRAS to study the CO + NO reaction on Pd(111) at elevated

pressures, we demonstrated the formation of NCO containing species and discussed some of the important implications of this observation regarding catalytic NO_x removal. These striking experimental results obtained by utilizing the powerful *in situ* capabilities of the PM-IRAS technique clearly emphasize the significance of studying heterogeneous catalytic reactions under realistic conditions such as elevated pressures and temperatures.

Acknowledgments

We acknowledge with pleasure the support of this work by the Department of Energy, Office of Basic Energy Sciences, Division of Chemical Sciences, and the R.A. Welch Foundation and the Texas Advanced Technology Program under Grant No. 010366-0022-2001. The authors would like acknowledge R.M. Lambert and N.W. Cant for fruitful discussions. C.H. thanks the Alexander von Humboldt foundation for providing a Feodor Lynen fellowship.

References

[1] R.M. Heck and R.J. Farrauto, Catalytic Air Pollution Control: *Commercial Technology*, (International Thomson Publishing, New York, NY, 1995).
[2] A.H. Tullo, Chem. Eng. News 80(34) (2002).
[3] B.D. Kay, C.H.F. Peden and D.W. Goodman, Phys. Rev. B 34 (1986) 817.
[4] C.H.F. Peden, B.D. Kay and D.W. Goodman, Surf. Sci. 175 (1986) 215.
[5] P.J. Berlowitz and D.W. Goodman, J. Catal. 108 (1987) 364.
[6] P.J. Berlowitz, C.H.F. Peden and D.W. Goodman, J. Phys. Chem. 92 (1988) 5213.
[7] W.K. Kuhn, J. Szanyi and D.W. Goodman, Surf. Sci. 274 (1992) L611.
[8] P.J. Chen and D.W. Goodman, Surf. Sci. 297 (1993) L93.
[9] J. Szanyi, W.K. Kuhn and D.W. Goodman, J. Vac. Sci. Technol. A—Vac. Surf. Films 11 (1993) 1969.
[10] X.P. Xu, P.J. Chen and D.W. Goodman, J. Phys. Chem. 98 (1994) 9242.
[11] J. Szanyi, W.K. Kuhn and D.W. Goodman, J. Phys. Chem. 98 (1994) 2978.
[12] J. Szanyi and D.W. Goodman, J. Phys. Chem. 98 (1994) 2972.
[13] S.M. Vesecky, P.J. Chen, X.P. Xu and D.W. Goodman, J. Vac. Sci. Technol. A—Vac. Surf. Films 13 (1995) 1539.
[14] S.M. Vesecky, D.R. Rainer and D.W. Goodman, J. Vac. Sci. Technol. A—Vac. Surf. Films 14 (1996) 1457.
[15] D.W. Goodman, J. Phys. Chem. 100 (1996) 13090.
[16] M. Bowker, R.P. Holroyd, R.G. Sharpe, J.S. Corneille, S.M. Francis and D.W. Goodman, Surf. Sci. 370 (1997) 113.
[17] E. Ozensoy, C. Hess and D.W. Goodman, J. Am. Chem. Soc. 124 (2002) 8524.
[18] A.K. Santra and D.W. Goodman, Electrochim. Acta 47 (2002) 3595.
[19] E. Ozensoy, D.C. Meier and D.W. Goodman, J. Phys. Chem. B 106 (2002) 9367.
[20] C. Hess, E. Ozensoy and D.W. Goodman, J. Phys. Chem. B 107 (2003) 2759.
[21] C. Xu and D.W. Goodman, Langmuir 12 (1996) 1807.
[22] C. Xu and D.W. Goodman, J. Phys. Chem. 100 (1996) 245.
[23] C. Xu and D.W. Goodman, J. Phys. Chem. B 102 (1998) 4392.
[24] J.A. Rodriguez and D.W. Goodman, J. Phys. Chem. 95 (1991) 4196.
[25] J.A. Rodriguez, R.A. Campbell and D.W. Goodman, Surf. Sci. 309 (1994) 377.
[26] R.A. Campbell, J.A. Rodriguez and D.W. Goodman, Phys. Rev. B 46 (1992) 7077.
[27] J.A. Rodriguez, R.A. Campbell and D.W. Goodman, J. Phys. Chem. 95 (1991) 5716.
[28] J.A. Rodruguez and D.W. Goodman, Science 257 (1992) 897.
[29] G. Liu, T.P. St Clair and D.W. Goodman, J. Phys. Chem. B 103 (1999) 8578.
[30] W.K. Kuhn, J. Szanyi and D.W. Goodman, Surf. Sci. 303 (1994) 377.
[31] W.K. Kuhn, J.W. He and D.W. Goodman, J. Vac. Sci. Technol. A—Vac. Surf. Films 10 (1992) 2477.
[32] P.J. Berlowitz and D.W. Goodman, Langmuir 4 (1988) 1091.
[33] D.R. Rainer, J.S. Corneille and D.W. Goodman, J. Vac. Sci. Technol. A—Vac. Surf. Films 13 (1995) 1595.
[34] X.P. Xu and D.W. Goodman, J. Phys. Chem. 97 (1993) 7711.
[35] J. Szanyi, X.P. Xu and D.W. Goodman, Abstracts Papers Am. Chem. Soc. 206 (1993) 83-ETR.
[36] X.P. Xu, J. Szanyi, Q. Xu and D.W. Goodman, Catal. Today 21 (1994) 57.
[37] X.P. Xu and D.W. Goodman, Catal. Lett. 24 (1994) 31.
[38] B.K. Min, A.K. Santra and D.W. Goodman, Appl. Catal., in press.
[39] B.K. Min, A.K. Santra and D.W. Goodman, J. Vac. Sci. Technol. A, in press.
[40] D.R. Rainer, M.C. Wu, D.I. Mahon and D.W. Goodman, J. Vac. Sci. Technol. A—Vac. Surf. Films 14 (1996) 1184.
[41] D.R. Rainer, C. Xu, P.M. Holmblad and D.W. Goodman, J. Vac. Sci. Technol. A—Vac. Surf. Films 15 (1997) 1653.
[42] D.R. Rainer, S.M. Vesecky, M. Koranne, W.S. Oh and D.W. Goodman, J. Catal. 167 (1997) 234.
[43] D.R. Rainer, M. Koranne, S.M. Vesecky and D.W. Goodman, J. Phys. Chem. B 101 (1997) 10769.
[44] P.M. Holmblad, D.R. Rainer and D.W. Goodman, J. Phys. Chem. B 101 (1997) 8883.
[45] Y.Q. Cai, A.M. Bradshaw, Q. Guo and D.W. Goodman, Surf. Sci. 399 (1998) L357.
[46] C. Xu, X. Lai, G.W. Zajac and D.W. Goodman, Phys. Rev. B 56 (1997) 13464.
[47] C. Xu, W.S. Oh, G. Liu, D.Y. Kim and D.W. Goodman, J. Vac. Sci. Technol. A—Vac. Surf. Films 15 (1997) 1261.
[48] X. Lai, T.P. St Clair, M. Valden and D.W. Goodman, Prog. Surf. Sci. 59 (1998) 25.
[49] C. Xu and D.W. Goodman, Chem. Phys. Lett. 263 (1996) 13.
[50] F.M. Hoffmann, Surf. Sci. Rep. 3 (1983) 107.
[51] D.W. Goodman, Surf. Rev. Lett. 2 (1995) 9.
[52] D.W. Goodman, Chem. Rev. 95 (1995) 523.
[53] R.D. Ramsier, Q. Gao, H.N. Waltenburg, K.W. Lee, O.W. Nooij, L. Lefferts and J.T. Yates, Surf. Sci. 320 (1994) 209.
[54] R.D. Ramsier, Q. Gao, H.N. Waltenburg and J.T. Yates, J. Chem. Phys. 100 (1994) 6837.
[55] M. Bertolo, K. Jacobi, S. Nettesheim, M. Wolf and E. Hasselbrink, Vacuum, 41 (1990) 76.
[56] M. Bertolo and K. Jacobi, Surf. Sci. 265 (1992) 12.
[57] *Electron Spectroscopy for Surface Analysis*, H. Ibach, J.D. Carette, *et al.* eds. (Springer-Verlag, Berlin, New York, 1977).
[58] G.A. Somorjai and K.R. McCrea, Adv. Catal. 45(45) (2000) 385.
[59] *Vibrational Spectroscopy of Molecules on Surfaces*, J.T. Yates eds. (Plenum Press, New York, 1987).
[60] T. Giessel, O. Schaff, C.J. Hirschmugl, V. Fernandez, K.M. Schindler, A. Theobald, S. Bao, R. Lindsay, W. Berndt, A.M.

Bradshaw, C. Baddeley, A.F. Lee, R.M. Lambert and D.P. Woodruff, Surf. Sci. 406 (1998) 90.
[61] V.V. Kaichev, I.P. Prosvirin, V.I. Bukhtiyarov, H. Unterhalt, G. Rupprechter and H.J. Freund, J. Phys. Chem. B 107 (2003) 3522.
[62] M.K. Rose, T. Mitsui, J. Dunphy, A. Borg, D.F. Ogletree, M. Salmeron and P. Sautet, Surf. Sci. 512 (2002) 48.
[63] G. Rupprechter, Phys. Chem. Chem. Phys. 3 (2001) 4621.
[64] G. Rupprechter, H. Unterhalt, M. Morkel, P. Galletto, L.J. Hu and H.J. Freund, Surf. Sci. 502 (2002) 109.
[65] S.G. Sugai, H. Watanabe, T. Kioka, H. Miki and K. Kawasaki, Surf. Sci. 259 (1991) 109.
[66] S. Surnev, M. Sock, M.G. Ramsey, F.P. Netzer, M. Wiklund, M. Borg and J.N. Andersen, Surf. Sci. 470 (2000) 171.
[67] G. Blyholder, J. Phys. Chem. 68 (1964) 2772.
[68] M.R. Albert, J. Catal. 195 (2000) 62.
[69] M. Bertolo and K. Jacobi, Surf. Sci. 236 (1990) 143.
[70] W.A. Brown and D.A. King, J. Phys. Chem. B 104 (2000) 2578.
[71] Q. Gao, R.D. Ramsier, H.N. Waltenburg and J.T. Yates, J. Am. Chem. Soc. 116 (1994) 3901.
[72] H. Conrad, G. Ertl, J. Kuppers and E.E. Latta, Surf. Sci. 65 (1977) 235.
[73] K.H. Hansen, Z. Sljivancanin, B. Hammer, E. Laegsgaard, F. Besenbacher and I. Stensgaard, Surf. Sci. 496 (2002).
[74] T.E. Hoost, K. Otto and K.A. Laframboise, J. Catal. 155 (1995) 303.
[75] M. Ikai and K. Tanaka, J. Chem. Phys. 110 (1999) 7031.
[76] A.J. Jaworowski, R. Asmundsson, P. Uvdal and A. Sandell, Surf. Sci. 501 (2002) 74.
[77] V. Johanek, S. Schauermann, M. Laurin, J. Libuda and H.J. Freund, Angew. Chem. Int. Ed. 42 (2003) 3035.
[78] C. Nyberg and P. Uvdal, Surf. Sci. 204 (1988) 517.
[79] S.W. Jorgensen, N.D.S. Canning and R.J. Madix, Surf. Sci. 179 (1987) 322.
[80] A.S. Mamede, G. Leclercq, E. Payen, P. Granger and J. Grimblot, J. Mol. Struct. 651 (2003) 353.
[81] I. Nakamura, T. Fujitani and H. Hamada, Surf. Sci. 514 (2002) 409.
[82] L. Piccolo and C.R. Henry, Surf. Sci. 452 (2000) 198.
[83] R.D. Ramsier, K.W. Lee and J.T. Yates, Surf. Sci. 322 (1995) 243.
[84] R. Raval, M.A. Harrison, S. Haq and D.A. King, Surf. Sci. 294 (1993) 10.
[85] Y.A. Aleksandrov, I.A. Vorozheikin, K.E. Ivanovskaya and D.G. Ivanov, Russ. J. Phys. Chem. 77 (2003) 202.
[86] K. Almusaiteer and S.S.C. Chuang, J. Catal. 180 (1998) 161.
[87] K. Almusaiteer and S.S.C. Chuang, J. Catal. 184 (1999) 189.
[88] M. Date, H. Okuyama, N. Takagi, M. Nishijima and T. Aruga, Surf. Sci. 350 (1996) 79.
[89] M. Date, H. Okuyama, N. Takagi and T. Aruga, Appl. Surf. Sci. 121 (1997) 571.
[90] R. Di Monte, J. Kaspar, P. Fornasiero, M. Graziani, C. Paze and G. Gubitosa, Inorg. Chim. Acta 334 (2002) 318.
[91] A. Elhamdaoui, G. Bergeret, J. Massardier, M. Primet and A. Renouprez, J. Catal. 148 (1994) 47.
[92] G.R. Garda, R.M. Ferullo and N.J. Castellani, Surf. Rev. Lett. 8 (2001) 641.
[93] G.W. Graham, A.D. Logan and M. Shelef, J. Phys. Chem. 97 (1993) 5445.
[94] M. Hirsimaki, S. Suhonen, J. Pere, M. Valden and M. Pessa, Surf. Sci. 404 (1998) 187.
[95] A.S. Mamede, G. Leclercq, E. Payen, P. Granger, L. Gengembre and J. Grimblot, Surf. Interface Anal. 34 (2002) 105.
[96] K. Nakao, H. Hayashi, H. Uetsuka, S. Ito, H. Onishi, K. Tomishige and K. Kunimori, Catal. Lett. 85 (2003) 213.
[97] L. Piccolo and C.R. Henry, Appl. Surf. Sci. 162 (2000) 670.
[98] L. Piccolo and C.R. Henry, J. Mol. Catal. A—Chem. 167 (2001) 181.
[99] G. Prevot, O. Meerson, L. Piccolo and C.R. Henry, J. Phys.—Condens. Matter 14 (2002) 4251.
[100] G. Prevot and C.R. Henry, J. Phys. Chem. B 106 (2002) 12191.
[101] M. Valden, J. Aaltonen, E. Kuusisto, M. Pessa and C.J. Barnes, Surf. Sci. 309 (1994) 193.
[102] M.J. Weaver, Surf. Sci. 437 (1999) 215.
[103] D.T. Wickham, B.A. Banse and B.E. Koel, Surf. Sci. 243 (1991) 83.
[104] C.T. Williams, A.A. Tolia, H.Y.H. Chan, C.G. Takoudis and M.J. Weaver, J. Catal. 163 (1996) 63.
[105] A.S. Worz, K. Judai, S. Abbet and U. Heiz, J. Am. Chem. Soc. 125 (2003) 7964.
[106] V.P. Zhdanov and B. Kasemo, Catal. Lett. 81 (2002) 141.
[107] B. Hammer and J.K. Norskov, Adv. Catal. 45 (45) (2000) 71.
[108] B. Hammer, J. Catal. 199 (2001) 171.
[109] B. Hammer, Phys. Rev. Lett. 89 (2002) art-016102.
[110] K. Honkala, P. Pirila and K. Laasonen, Phys. Rev. Lett. 86 (2001) 5942.
[111] K. Honkala, P. Pirila and K. Laasonen, Surf. Sci. 489 (2001) 72.
[112] M.P. Jigato, K. Somasundram, V. Termath, N.C. Handy and D.A. King, Surf. Sci. 380 (1997) 83.
[113] Z.P. Liu and P. Hu, J. Am. Chem. Soc. 125 (2003) 1958.
[114] D. Loffreda, D. Simon and P. Sautet, Chem. Phys. Lett. 291 (1998) 15.
[115] D. Loffreda, D. Simon and P. Sautet, J. Chem. Phys. 108 (1998) 6447.
[116] D. Loffreda, D. Simon and P. Sautet, Surf. Sci. 425 (1999) 68.
[117] D. Loffreda, F. Delbecq, D. Simon and P. Sautet, J. Chem. Phys. 115 (2001) 8101.
[118] D. Loffreda, D. Simon and P. Sautet, J. Catal. 213 (2003) 211.
[119] M.C. Asensio, D.P. Woodruff, A.W. Robinson, K.M. Schindler, P. Gardner, D. Ricken, A.M. Bradshaw, J.C. Conesa and A.R. Gonzalezelipe, Chem. Phys. Lett. 192 (1992) 259.
[120] R. Raval, Surf. Sci. 333 (1995) 1.
[121] M. Bertolo and K. Jacobi, Surf. Sci. 226 (1990) 207.
[122] A. Eichler, Surf. Sci. 526 (2003) 332.
[123] G.W. Smith and E.A. Carter, J. Phys. Chem. 95 (1991) 2327.
[124] S.M. Vesecky, Ph.D.Thesis (Texas A&M University, College Station, 1996).
[125] M.L. Unland, Science 179 (1973) 567.
[126] M.L. Unland, J. Catal. 31 (1973) 459.
[127] N. Macleod and R.M. Lambert, Chem. Commun. (2003) 1300.
[128] D.C. Chambers, D.E. Angove and N.W. Cant, J. Catal. 204 (2001) 11.
[129] N.W. Cant, D.C. Chambers and I.O.Y. Liu, Appl. Catal. B—Environ., in press.
[130] F. Solymosi and T. Bansagi, J. Catal. 202 (2001) 205.
[131] H. Celio, K. Mudalige, P. Mills and M. Trenary, Surf. Sci. 394 (1997) L168.